

Interferential formulization and interpretation of the photoacoustic effect in multi-layered cells

Jinan Cao†

Department of Organic and Polymeric Materials, Tokyo Institute of Technology, Tokyo, Japan

E-mail: jinan.cao@tft.csiro.au

Received 29 October 1999

Abstract. Mathematical formulization of the thermal response in a two-layer photoacoustic cell, where the interference of thermal waves in a sample is compounded by the inter-layer interference effect, has been carried out by employing the thermal-wave interference theory. The physical meanings of the obtained formulae are then discussed in terms of the thermal-wave interference to explain the origin of the thermal phase lag for various cases. In addition, it is found that the inter-layer thermal-wave interference results in an extra phase lag.

1. Introduction

In a cell for photoacoustic effect (PAE), a sample absorbs modulated light and converts it into thermal waves. The thermal waves travel forward and backward, and strike the rear and front surfaces of the sample. Periodical temperature variations on the sample surfaces make the air boundary layer intimately contacting the surfaces expand and contract periodically, forming a sound wave spreading everywhere in the cell. A microphone detects the sound signal as output. While a microphone is mounted on the same side as the illuminated surface of the sample for a front-surface technique, it is mounted on the backside for a rear-surface PAE cell, as shown in figure 1 [1–6].

The phase lag of the sound signal relative to the modulated light signal as detected by the microphone is particularly useful to determine the thermal diffusivity of a sample. The converting time of the modulated light to heat upon its absorption is believed to be far shorter than 10^{-9} s. The phase lag of the sound signal relative to the modulated light is, therefore, dominated by the travelling time of the thermal waves to the surfaces of the sample, and the travelling time of the sound wave from the surfaces of the sample to the microphone [6]. The phase lag between the temperature variation on the surfaces of a sample and the modulated light may be termed the thermal phase lag; and the phase lag between the temperature variation and the sound signal can be called the sound phase lag. What is measured in a photoacoustic experiment is the sum of the thermal phase lag and the sound phase lag [6]. In this study, only the thermal phase lag is addressed.

† Present address: CSIRO Division of Wool Technology, PO Box 21, Belmont, Victoria 3216, Australia

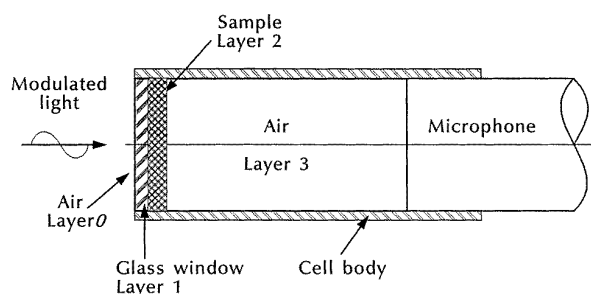


Figure 1. A model photoacoustic cell for the rear-surface technique.

There are two main approaches to derive equations relating the thermal phase lag to the thermal properties of a sample. One is the approach, by which the thermal diffusion differential equation is solved by combining with various boundary conditions. This approach has led to the establishment of the Rosencwaig–Gersho theory (RG theory) [1, 2, 7–10], which accounts for the relationship between the temperature variation and the thermal properties for the front-surface technique. Charpentier *et al* [11] expanded the RG theory to include the rear-surface technique. The other, presented by Bennett and Patty [12], formulized the thermal response as a superposition of thermal waves on the sample surface using interference theory, and recast the RG theory. Several authors have since discussed thermal-wave interference and diffraction [13, 14]. The former approach is applicable to all cases whenever boundary conditions can be expressed mathematically. On the other hand, the latter is much simpler in mathematics, but appears to be applicable only to some special cases.

The present paper will show, in particular, that the concept of thermal-wave interference can be employed to offer a physical interpretation for the thermal response in photoacoustic cells, which could permit a transfer of many methodologies developed for interference optics to PAE studies.

A multi-layered cell is employed in this study to include the inter-layer interference effect. There was only intra-layer interference effect in the Bennett and Patty model because they assumed that the backing material was infinitely thick; neither was the rear-surface illumination technique addressed. To simplify the mathematical manipulations and to place emphasis on the physical meanings only one-dimensional heat flow is considered in this study. Further assumptions are: the glass window is assumed to be completely transparent, absorbing no modulated light; the surface of a sample is supposed to be a complete black body; and a thermal wave is generated on the surface upon its absorption of the modulated light. The PAE configuration shown in figure 1 was studied by Adams and Kirkbright and an equation relating the thermal phase lag to the thermal diffusivity of samples was derived by solving the differential diffusion equation [1, 2].

There are both intra- and inter-layer interferences for such a cell. The relationship between the temperature variation and the thermal diffusivity of a sample will be derived using the thermal-wave interference theory. The origin of the thermal phase lag is then interpreted in terms of the thermal-wave interference.

2. Formulism of the temperature variation on the rear-surface

For convenience and generality of this discussion, from here on the glass, sample and air in the photoacoustic cell are called layer 1, layer 2 and layer 3, respectively, as shown in figure 1.

Now consider interference behaviour of a unit thermal wave, I , which is generated upon its absorption of the modulated light on the sample surface. Half of this thermal wave should diffuse leftward and half should travel rightward in a thermally homogeneous material. However, part of the leftward half will reflect off the glass sample interface, S_{12} . As a result, one obtains the rightward portion $I_2 = (1 + R_{21})I/2$ and leftward portions $I_1 = T_{21}I/2$, where, R_{21} and T_{21} are the thermal-wave reflection coefficient and transmission coefficient from layer 2 to layer 1, respectively.

As I_2 impinges at interface S_{23} , part of it will transmit into the air layer intimately contacting the sample surface and part of it should reflect off the interface and travel back toward interface S_{12} . The reflected portion of the thermal wave will further split into two parts when it arrives at S_{12} ; one reflects off interface S_{12} and the other emits into the glass window. At the same time, part of I_1 will reflect off interface S_{01} as soon as the thermal wave I_1 arrives at the interface. A portion of the thermal wave, which is reflected off interface S_{01} , shall penetrate interface S_{12} to interfere with the thermal waves in the sample layer. This type of transmission and reflection continues until the thermal waves are completely damped. The temperature variation on the rear surface of the sample

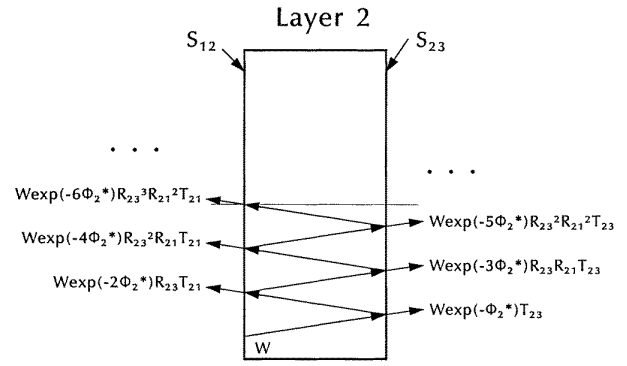


Figure 2. Sub-superposition of selected thermal waves.

(the surface contacting air), which in turn results in sound waves, should be the superposition of these thermal waves.

Thus, not only the thermal waves resulting from multiple reflections in layer 2, but also the thermal waves re-entering layer 2 from layer 1 should be accounted for. By contrast, only the thermal waves resulting from multiple reflections in layer 2 were taken into consideration in Bennett and Patty's paper. To obtain the superposition for the complicated thermal waves, one may sum the thermal waves by two separate manipulations in which the thermal waves are sub-superposed and then superposed as follows.

2.1. Sub-superposition of selected thermal waves

First let us calculate the sub-superposition of the thermal waves entering the air layer and the sub-superposition of the thermal waves entering the glass window when a thermal wave, ($W = W_0 \sin(\omega t)$) at interface S_{12} , travels toward interface S_{23} from the front surface of a sample without taking into consideration the thermal waves bouncing back from the glass window, as shown in figure 2.

The thermal wave is damped to become $W_0 \sin(\omega t) \exp(-\varphi_2^*)$ as it strikes Interface, S_{23} . Part of it, $W_0 \sin(\omega t) \exp(-\varphi_2^*)T_{23}$, emits into the air layer whilst the other part, $W_0 \sin(\omega t) \exp(-\varphi_2^*)R_{23}$, reflects off the interface. Here, the symbols R and T represent the emission coefficient and the reflection coefficient, respectively; the subscript 23 denotes that the emission or reflection is from layer 2 to layer 3. The emission of the thermal wave into layer 3 occurs again when $W_0 \sin(\omega t) \exp(-\varphi_2^*)R_{23}$ has returned to interface S_{23} . The thermal-wave fraction entering layer 3 is written as, $W_0 \sin(\omega t) \exp(-3\varphi_2^*)R_{23}R_{21}T_{23}$. If calling the above mentioned thermal waves emitting into layer 3 the first wave and the second wave, respectively, one can readily work out expressions for higher waves.

According to Bennett and Patty, the complex number relating to the damping and phase lag behaviour of the thermal waves, φ_2^* , is written [12]

$$\varphi_2^* = (1 + j)\varphi_2 = (1 + j)\sqrt{\frac{\omega}{2\alpha_2}}l_2 \quad (1)$$

where ω is the modulation frequency of light and α_2 and l_2 are the thermal diffusivity and the thickness of layer 2, respectively. The complex number φ_2^* describes the change of the thermal wave when travelling through layer 2. Its real part

is related to the attenuation of the amplitude (from $W_0 \sin(\omega t)$ to $W_0 \sin(\omega t) \exp(-\varphi_2)$) and its imaginary part gives the phase lag.

The sub-superposition of the thermal waves can be obtained by summing up all of the thermal waves emitting from the rear-surface of the sample into the air layer, which form a geometric series.

$$W_0 \exp(-\varphi_2^*) T_{23} + W_0 R_{23} R_{21} \exp(-3\varphi_2^*) T_{23} + W_0 R_{23}^2 R_{21}^2 \exp(-5\varphi_2^*) T_{23} + \dots \quad (2)$$

If the transmission coefficient for the rightward wave advancing from layer 2 (the right-hand side of interface S_{12}) into layer 3 (the right-hand side of interface S_{23}) is termed A_2 , one obtains

$$A_2 = [T_{23} \exp(-\varphi_2^*)] \left(\frac{1}{1 - R_{23} R_{21} \exp(-2\varphi_2^*)} \right) \quad (3)$$

where the subscript 2 denotes layer 2.

This formula is similar to that for the light interference in a Fabry–Perot interferometer [15]. In the same manner, one may obtain the sub-superposition of the thermal waves entering the glass window which result from multiple reflections and emissions of the primary thermal wave, W . The transmission coefficient for the rightward wave backing to layer 1 (left-hand side of interface S_{12}), B_2 , is given by

$$B_2 = R_{23} T_{21} \exp(-2\varphi_2^*) \frac{1}{1 - R_{23} R_{21} \exp(-2\varphi_2^*)}. \quad (4)$$

The sub-superposition of the thermal waves entering layer 2, which result from a primary thermal wave travelling in layer 1 from interface S_{12} , B_1 , is written

$$B_1 = R_{10} T_{12} \exp(-2\varphi_1^*) \frac{1}{1 - R_{10} R_{12} \exp(-2\varphi_1^*)} \quad (5)$$

where φ_1^* in equation (5) is the decay factor of layer 1 and is given by

$$\varphi_1^* = (1 + j)\varphi_1 = (1 + j)\sqrt{\frac{\omega}{2\alpha_1}} l_1. \quad (6)$$

Equations (3)–(5) are the three sub-superpositions required to obtain the total superposition.

2.2. Temperature variation on the rear surface of a sample

In the same method adopted to obtain the sub-superposition in section 2.1, one may readily obtain the mathematical expression of the temperature variation on the rear surface of a sample. Figure 3 shows how this temperature variation can be calculated. For I_2 , it is obvious that $I_2 A_2$ will be a sub-superposition emitting into layer 3. At the same time there is $I_2 B_2$ entering the glass window, therefore $(I_1 + I_2 B_2)$ can be considered to be a primary wave travelling toward interface S_{01} . By applying the B operation to layer 1, one realizes that the thermal wave, $(I_1 + I_2 B_2) B_1$, should enter the sample layer. The thermal wave entering layer 3 due to this thermal wave is written as $(I_1 + I_2 B_2) B_1 A_2$. Therefore,

the temperature variation on the rear-surface of the sample intimately contacting the adjacent air layer is written

$$\begin{aligned} I_{rear} &= I_2 A_2 + (I_1 + I_2 B_2) B_1 A_2 + (I_1 + I_2 B_2) B_1^2 B_2 A_2 \\ &\quad + (I_1 + I_2 B_2) B_1^3 B_2^2 A_2 + \dots \\ &= I_2 A_2 + \frac{(I_1 + I_2 B_2) B_1 A_2}{1 - B_1 B_2} = A_2 \left(\frac{I_2 + I_1 B_1}{1 - B_1 B_2} \right) \\ &= \{T_{23} \exp(-\varphi_2^*)\} \left\{ \frac{1}{1 - R_{23} R_{21} \exp(-2\varphi_2^*)} \right\} \\ &\quad \times \left\{ \frac{I_2 + I_1 B_1}{1 - B_1 B_2} \right\} \end{aligned} \quad (7)$$

where the reflection coefficient and transmission coefficient are calculated as follows [12]:

$$R_{ij} = \frac{1 - b_{ij}}{1 + b_{ij}} \quad (8)$$

$$T_{ij} = 1 - R_{ij} \quad (9)$$

where b_{ij} is the ratio of the effusivities, e_i and e_j , which are defined in equation (11)

$$b_{ij} = \frac{1/e_i}{1/e_j} = \frac{e_j}{e_i} \quad (10)$$

$$e = \sqrt{\rho C k} \quad (11)$$

where the symbols ρ , C and k represent the density, heat capacity and thermal conductivity of a layer, respectively.

Equation (7) is the formula of the temperature variation on the rear surface of a sample.

3. Interpretation of the thermal phase lag by the thermal wave interference theory

3.1. Physical meanings and their corresponding components

Equation (7) shows that the total phase lag between the temperature variation on the rear surface of a sample and the modulated light consists of three terms, separated by the three brackets. The first term shows the phase lag and intensity corresponding to the first wave of the primary wave. The second term represents the interference effect of the thermal waves reflecting off the interfaces, S_{12} and S_{23} , therefore intra-layer interference. The third term in equation (7) denotes an additional phase lag resulting from the interference effect of the thermal waves re-entering from layer 1 into layer 2, therefore inter-layer interference. This term is absent in the equation derived by Charpentier *et al* [11]. The interference effects result in additional phase lags.

3.2. Numerical calculation and quantitative analysis

The phase lag and intensity of the temperature variation on the rear surface of a sample can be readily calculated according to equation (7). The intensity is simply the product and the phase lag the sum of the three terms shown in equation (7). To reduce the number of independent variables, the author has calculated the phase lag ($\Delta\theta$) and intensity against φ_2 , which is further converted into degrees by multiplying by $180/\pi$, at a given φ_1/φ_2 ratio and R_{21} . φ_1 and φ_2 are

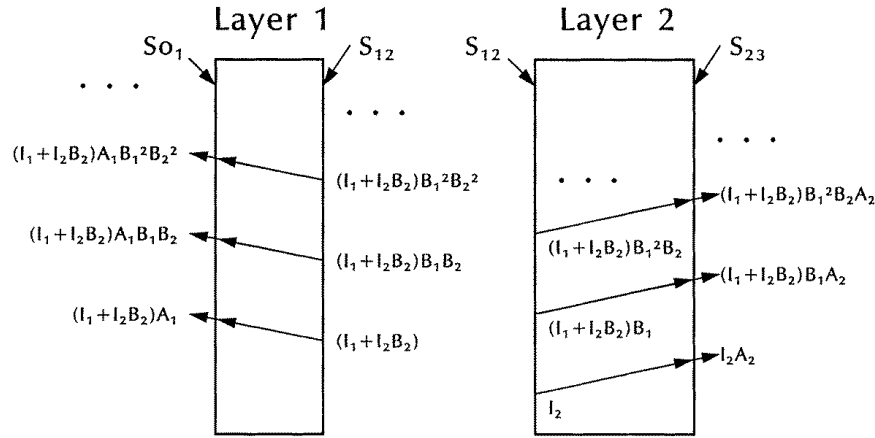


Figure 3. Superposition of the thermal waves on the rear surface of the sample, S_{23} .

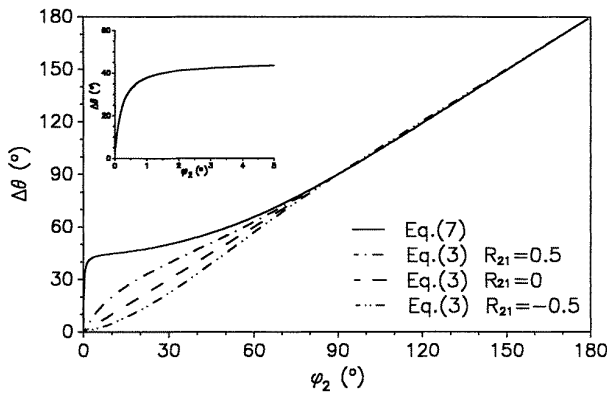


Figure 4. The numerical results of the thermal phase lag, $\Delta\theta$, against the thermal thickness of a sample for equations (7) and (3), when layer 1 and layer 2 have the same thermal thickness ($\varphi_1/\varphi_2 = 1$). The insert shows the curve with expanded abscissa at the low- φ_2 region.

defined in equations (1) and (6) respectively. The reflection coefficients R_{10} and R_{23} were determined by taking the physical properties in table 1 into consideration. Clearly, R_{10} and R_{23} do not change a great deal, hence, $R_{10} = R_{23} = 0.99$ was adopted to obtain figures 4–9. A QBASIC computer program is attached in the appendix to permit one to calculate any specific curve not shown in this paper.

Figures 4 and 5 show the thermal phase lag, $\Delta\theta$, and the intensity for three different reflection coefficients $R_{21} = 0.5, 0, -0.5$, when layer 1 and layer 2 have the same thermal thickness ($\varphi_1/\varphi_2 = 1$). The three curves for equation (7) overlap and are almost indistinguishable in figure 4. The difference between the curves for equation (7) and the curves for equation (3) represents the extra phase lag resulting from the inter-layer interference. This extra phase lag is gradually eliminated with an increase in the thermal thickness (increasing either the frequency of the modulated light or the sample thickness). Both equation (7) and equation (3) start from the origin (see the insert) and approach the straight line of $\Delta\theta = \varphi_2$, indicating that only the phase lag of the first wave needs to be considered at high φ_2 region. This is a result of the damping effect of the thermal waves; higher thermal waves become negligible compared with the first wave.

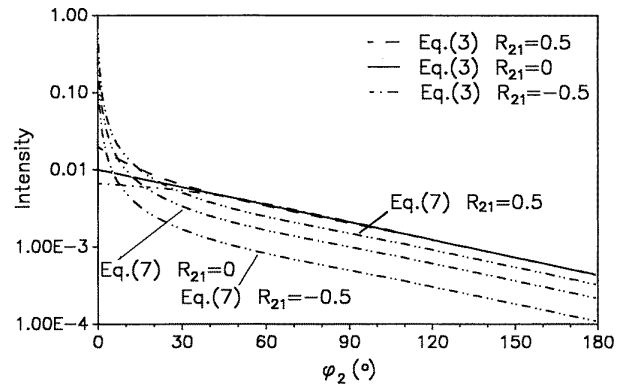


Figure 5. The numerical results of the intensity against the thermal thickness of a sample for equations (7) and (3), when layer 1 and layer 2 have the same thermal thickness ($\varphi_1/\varphi_2 = 1$).

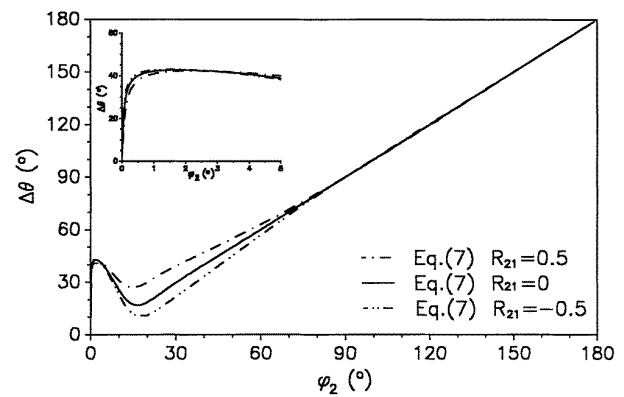


Figure 6. The numerical results of the thermal phase lag, $\Delta\theta$, against the thermal thickness of a sample for equation (7), where $\varphi_1/\varphi_2 = 5$.

The intensity curve shown in figure 5 can be interpreted as follows. At low φ_2 region, significant inter-layer interference effect results in a higher intensity for equation (7) than for equation (3). However as φ_2 increases, the first wave, whose portion is determined by R_{21} , gradually becomes the major contribution to the total intensity. A lower intensity for equation (7) than for equation (3) is expected. Indeed, the intensity curve for equation (7) overlaps with the curve of equation (3) when R_{21} approaches unity.

Table 1. The physical properties of some materials [16].

Element	ρ	C	k
O ₂	0.04 (mol l ⁻¹)	21.1 J mol ⁻¹ °C ⁻¹	26.3 mW m ⁻¹ °C ⁻¹
Al	2730 g l ⁻¹	0.215 × 4.18 J g ⁻¹ °C ⁻¹	2370 mW cm ⁻¹ °C ⁻¹

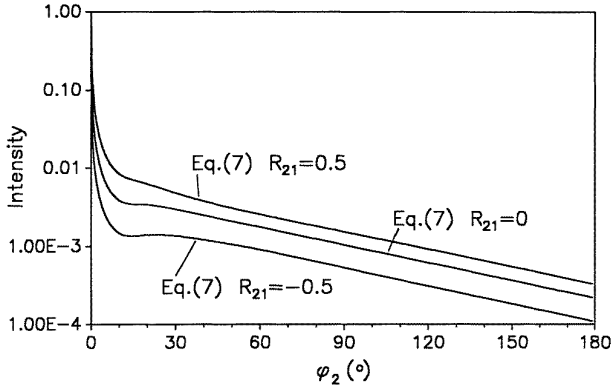


Figure 7. The numerical results of the intensity against the thermal thickness of a sample for equation (7), where $\varphi_1/\varphi_2 = 5$.

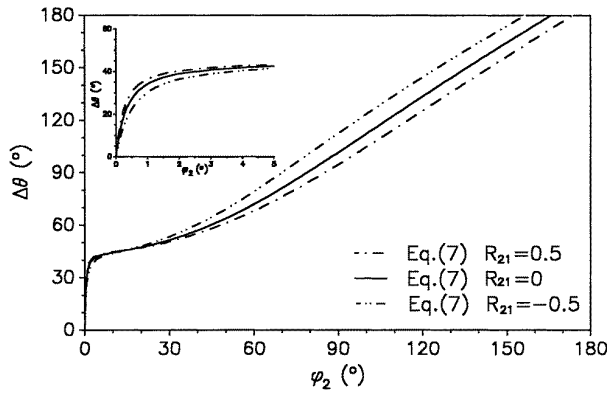


Figure 8. The numerical results of the thermal phase lag, $\Delta\theta$, against the thermal thickness of a sample for equation (7), where $\varphi_1/\varphi_2 = 0.2$.

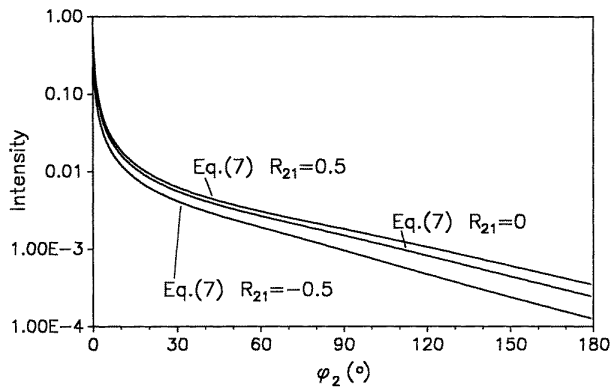


Figure 9. The numerical results of the intensity against the thermal thickness of a sample for equation (7), where $\varphi_1/\varphi_2 = 0.2$.

Figures 6 and 7 show the curves similar to figure 4 and 5 but for the case of $\varphi_1/\varphi_2 = 5$, where layer 1 is, thermally, five times, thicker than layer 2. The phase lag

starts from zero at the origin, initially shows a quick increase, reaches a maximum, drops to a minimum then increases with increasing φ_2 monotonically. The corresponding intensity curves in figure 7, in particular for the case of $R_{21} = -0.5$, shows a clear maximum and minimum, a characteristic phenomenon of interference. The extra phase lag is seen to be eliminated at a much lower thermally thin region than in the case of $\varphi_1/\varphi_2 = 1$ (figure 4). This is caused by the stronger thermal damping effect of layer 1. Note that equation (3) is irrelevant to the φ_1/φ_2 ratio, the curves are identical with those displayed in figures 4 and 5.

Figures 8 and 9 show the phase lag and intensity curves for the case of $\varphi_1/\varphi_2 = 0.2$, where layer 1 is, thermally, five times thinner than layer 2. Both the phase lag and intensity curves show similar features to those shown in figures 4 and 5. However, the phase lag does not approach the straight line of $\Delta\theta = \varphi_2$, instead a constant additional phase lag is retained at the high φ_2 region. This is because the contribution from inter-layer interference becomes significant, compared with the first wave and the intra-layer interference component, which is evident by the higher intensity in figure 9 than that in figure 5. Indeed, it is the ratio of these components and their relative phases that determine the total phase lag and intensity.

3.3. Recasting equations for single-layer model

In the situation where $e_1 = e_2$, layer 1 and layer 2 are thermally indistinguishable. Thus there is no reflection on the interface of layer 1 and layer 2. One shall expect no inter-layer interference effect. It turns into a single-layer model in this case, but the initial thermal wave is generated inside the layer rather than on the surface. Where $b_{21} = 1$, other parameters read:

$$R_{21} = 0 \quad T_{21} = 1 \quad R_{12} = 0 \quad T_{12} = 1$$

and

$$I_1 = I_0/2 \quad I_2 = I_0/2.$$

By substituting these parameters together with equations (4) and (5) for B_1 and B_2 into equation (7), one obtains

$$\begin{aligned}
 I_{rear} &= (T_{23} \exp(-\varphi_2^*)) (1) \\
 &\times \left(\frac{\frac{1}{2} + \frac{1}{2} R_{10} T_{12} \exp(-2\varphi_1^*)}{1 - T_{12} T_{21} R_{10} R_{23} \exp[-2(\varphi_1^* + \varphi_2^*)]} \right) \\
 &= \frac{1}{2} (T_{23} \exp(-\varphi_2^*)) \left(\frac{1}{1 - R_{10} R_{23} \exp[-2(\varphi_1^* + \varphi_2^*)]} \right) \\
 &+ \frac{1}{2} R_{10} \{ T_{23} \exp[-(\varphi_2^* + 2\varphi_1^*)] \} \\
 &\times \left(\frac{1}{1 - R_{10} R_{23} \exp[-2(\varphi_1^* + \varphi_2^*)]} \right). \tag{12}
 \end{aligned}$$

Equation (12) indicates that the inter-layer interference turns into the intra-layer interference. It consists of two

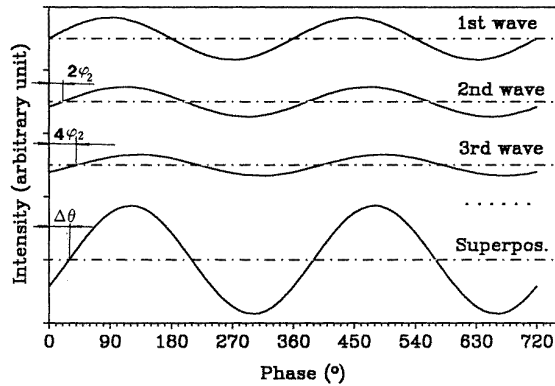


Figure 10. Schematic illustration for the thermal phase lag in the front surface of a sample.

components corresponding to the half of the primary wave initially travelling toward layer 2; and the half initially travelling toward layer 1 upon its generation. The intra-layer interference terms are identical for the two components. Equation (12) has been used to calculate the phase lag and intensity and it produces the same results as those shown in figures 4–9, which were obtained using equation (7). Equation (12) turns into the true equation for a normal single-layer model in the case of $\varphi_1 = 0$ (R_{21} in equation (3) turns into R_{10}).

3.4. Interpretation of the thermal phase lag in the front-surface technique

The above methodology can be applied to obtain the corresponding formula for the front-surface technique by considering layer 1 as an air layer and assuming it to be thermally so thick that the interference effect from the thermal waves reflected from the interface, S_{01} , can be neglected. Summing up all of the thermal waves on the front surface of the sample, which form a geometric series, leads to the expression of the temperature variation on the front surface of the sample (cf equation (3)):

$$I_{front} = T_{21} R_{23} \frac{1}{1 - R_{23} R_{21} \exp(-2\varphi_2^*)}. \quad (13)$$

This equation indicates that the phase lag for a front-surface technique, originates purely from the interference effect of the thermal waves reflecting off the interfaces, S_{12} and S_{23} , since there is no phase lag for the first wave in this case.

The above explanation can be further illustrated by using figure 10. The first thermal wave, which is generated upon the absorption of the modulated light by a sample, should have no phase lag relative to the light signal. It is the second thermal wave and the higher waves that show the phase lags after their multiple travels between the interfaces, S_{12} and S_{23} . The temperature variation on the surface of a sample is the superposition of the first, second and higher thermal waves. The origin of the phase lag in a front-surface arrangement lies in the intra-layer interference effect. Thus for a thermally thick sample, the second and higher waves are so damped that little contribution to the superposition could be anticipated.

The phase lag approaches zero. This explains why the phase lag for the front-surface technique has a maximum with an increase in the modulation frequency.

3.5. Application range of the Adams and Kirkbright equation

Adams and Kirkbright studied the rear-surface technique and derived a formula by solving the diffusion equation in the late 1970s, which suggested $\Delta\theta = \varphi_2$ (the first term of equation (7)) for the whole frequency range [1, 2]. It was comprehensive and basically a principle-proof type of work. The boundary condition in their paper, i.e. the temperature variation on the front surface (see also equation (3) and figure 3 in [1]), was assumed to have the same phase as the modulated light. Thus the Adams and Kirkbright equation is only applicable to the thermally thick range, as the boundary condition is only true when the intra- and inter-layer interference effects are negligible, which has been discussed in section 3.4.

3.6. Recasting the Charpentier *et al* equation

There is another special case worthy of mention in which the interference effect from layer 1 is negligible. If the effusivity ratio of layer 1 to layer 2 approaches zero, no thermal waves would emit into layer 1 from layer 2. This fact indicates that no interference effect of the thermal waves from layer 1 should be considered, no matter whether layer 1 and layer 2 are thermally thin or not. This can be further manifested by the following mathematical manipulations. When $b_{21} = 0$, one obtains

$$R_{21} = 1 \quad T_{21} = 0 \quad R_{12} = -1 \quad T_{12} = 2$$

and

$$I_1 = 0 \quad I_2 = I \quad B_2 = 0.$$

Therefore the third term in equation (7) becomes unity; equation (7) becomes identical to equation (3) and the relationship derived by Charpentier *et al* is retrieved.

4. Conclusion

The temperature variation on the rear surface of a sample in a two-layered photoacoustic cell, where both the intra- and inter-layer thermal-wave interferences have to be taken into account, has been formulized by employing the thermal-wave interference theory. The obtained formulae are consistent with those in literature, which were obtained by solving the thermal diffusion differential equation. It is found that if the glass window is thermally thin and the ratio of the thermal effusivities of a sample to the glass window is not negligible, there is an extra phase lag resulting from the inter-layer interference effect of the thermal waves. In addition, the physical origin of the phase lags is interpreted consistently in terms of the thermal waves travelling and their interference effects.

Appendix. A Qbasic computer program

```

10 ' *** define functions and constants ***
20 drc = 180 / 3.141592
30 ' ** phase and int. for function: x + y exp((j+1)z) **
40 DEF fnphc (x, y, z) = ATN(y * EXP(z) * SIN(z))
  / (x + y * EXP(z) * COS(z))
50 DEF fninc (x, y, z) = SQR(x * x + y * y * EXP(2 * z)
  + 2 * x * y * EXP(z) * COS(z))
60 ' ** phase and int. for function: x + y exp(jz) **
70 DEF fnph (x, y, z) = ATN(y * SIN(z) / (x + y * COS(z)))
80 DEF fnin (x, y, z) = SQR(x * x + y * y + 2 * x * y * COS(z))
100 '
110 ' *** main ***
120 ' ** input independent variables **
130 R10 = .99: R23 = .99: T10 = 1 - R10: T23 = 1 - R23
140 INPUT "Please input R21 = "; R21
150 INPUT " Please input r.phi1/phi2 = "; r.phi1.phi2
160 INPUT " Please input file name for output data; "; fl
170 OPEN fl FOR OUTPUT AS #1
180 '
190 ' ** calculate dependent variables **
200 B21 = (1 - R21) / (1 + R21)
210 T21 = 1 - R21
220 R12 = -R21: T12 = 1 - R12
230 I0 = 1: I1 = T21 / 2 * I0: I2 = (1 + R21) / 2 * I0
240 '
250 ' ** main calculation (loop) **
260 d.phi2 = 0
270 phi2 = d.phi2 / drc ' deg.gra conversion *
280 phi1 = phi2 * r.phi1.phi2
290 '
300 GOSUB 1000 ' * obtain phase and intensity *
310 '
320 PRINT d.phi2; delta.eq7; delta.A2, inten.eq7; inten.A2
330 PRINT #1, d.phi2, delta.eq7, delta.A2, inten.eq7, inten.A2
340 IF d.phi2 <= 2 THEN stp = .01 ELSE stp = 1
350 d.phi2 = d.phi2 + stp
360 IF d.phi2 > 180 GOTO 500
370 GOTO 270
500 CLOSE #1
990 END
999 '
1000 ' ** subroutine for phase and intensity **
1010 ' * obtain A2 (equation^3)
1020 delta2 = fnphc(1, -R23 * R21, -2 * phi2)
1030 inten2 = fninc(1, -R23 * R21, -2 * phi2)
1040 ' * obtain B1
1050 B1denom.in = fninc(1, -R10 * R12, -2 * phi1)
1060 B1denom.ph = fnphc(1, -R10 * R12, -2 * phi1)
1070 B1in = T12 * R10 * EXP(-2 * phi1) / B1denom.in
1080 B1ph = (-2 * phi1) - B1denom.ph
1090 ' * obtain B2
1100 B2in = R23 * T21 * EXP(-2 * phi2) / inten2
1120 B2ph = (-2 * phi2) - delta2
1130 ' * obtain (I2+I1 B1)
1140 delta3 = fnph(I2, I1 * B1in, B1ph)
1150 inten3 = fnin(I2, I1 * B1in, B1ph)
1160 ' * obtain (1-B1 B2)
1180 B1B2in = B1in * B2in: B1B2ph = B1ph + B2ph
1190 inten4 = fnin(1, -B1B2in, B1B2ph)
1200 delta4 = fnph(1, -B1B2in, B1B2ph)
1210 '
1220 delta.eq7 = -(-phi2 - delta2 + delta3 - delta4) * drc
1230 delta.A2 = -(-phi2 - delta2) * drc
1240 inten.eq7 = T23 * EXP(-phi2) / inten2 * inten3 / inten4
1250 inten.A2 = T23 * EXP(-phi2) / inten2
1300 RETURN

```

References

- [1] Adams M J and Kirkbright G F 1977 *Analyst* **102** 281
- [2] Adams M J and Kirkbright G F 1977 *Analyst* **102** 678
- [3] Swimm R T 1983 *Appl. Phys. Lett.* **42** 955
- [4] Lachaine A and Poulet P 1984 *Appl. Phys. Lett.* **45** 953
- [5] Pessoa O, Cesar C L Jr, Patel N A, Varges H, Ghizoni C C and Miranda L C M 1986 *J. Appl. Phys.* **59** 1316
- [6] Hashimoto T, Cao J and Takaku A 1987 *Thermochim. Acta* **120** 191
- [7] Rosencwaig A and Gersho A 1976 *J. Appl. Phys.* **47** 64
- [8] McDonald F A and Wetsel G C Jr 1978 *J. Appl. Phys.* **49** 2313
- [9] McDonald F A 1980 *Appl. Phys. Lett.* **36** 123
- [10] Fujii Y, Moritani A and Nakai J 1981 *Japan. J. Appl. Phys.* **20** 361
- [11] Charpentier P, Lepoutre F and Bertrand L 1982 *J. Appl. Phys.* **53** 608
- [12] Bennett C A Jr and Patty R R 1982 *Appl. Opt.* **21** 49
- [13] Mandelis A 1989 *J. Opt. Soc. Am. A* **6** 298
- [14] Mandelis A and Leung K F 1991 *J. Opt. Soc. Am. A* **8** 186
- [15] for example Lapedes D N 1977 *McGraw-Hill Dictionary of Scientific and Technical Terms* (New York: McGraw-Hill)
- [16] Lide D R 1990 *CRC Handbook of Chemistry and Physics* 71st edn (Boca Raton, FL: CRC Press)